Surgivisio® and O-arm®O2 cone beam CT mobile systems for guidance of lumbar spine surgery: Comparison of patient radiation dose

Julia Rousseau, Serge Dreuil, Celine Bassinet, Sophie Cao, Hélène Elleaume

Surgivisio® and O-arm®O2 cone beam CT mobile systems for guidance of lumbar spine surgery: Comparison of patient radiation dose

Julia Rousseau[a], Serge Dreuil[b], Céline Bassinet[b], Sophie Cao[c] and Hélène Elleaume[d].

Affiliation and addresses :

[a] Pôle imagerie, CHU Grenoble Alpes, Avenue Maquis du Grésivaudan, 38700 La Tronche, France.

[b] Institut de Radioprotection et de Sûreté Nucléaire (IRSN), 31 Avenue de la Division Leclerc, 92260 Fontenay-aux-Roses, France.

[c] Pôle Coordination des Gestes Chirurgicaux et Interventionnels, CHU Grenoble Alpes, Avenue Maquis du Grésivaudan, 38700 La Tronche, France.

[d] INSERM UA07 Team STROBE, ESRF 71 Avenue des Martyrs, 38000 Grenoble, France.

E-mail addresses:

Julia Rousseau : jrousseau@chu-grenoble.fr

Serge Dreuil : serge.dreuil@irsn.fr

Céline Bassinet : celine.bassinet@irsn.fr

Sophie Cao : scao@chu-grenoble.fr

Hélène Elleaume : Helene.elleaume@inserm.fr

Corresponding author:

Julia Rousseau

Declarations of interest: none

Article Title

Surgivisio® and O-arm®O2 cone beam CT mobile systems for guidance of lumbar spine surgery: Comparison of patient radiation dose

Abstract

Purpose: To compare patient radiation doses in cone beam computed tomography (CBCT) of two mobile systems used for navigation-assisted mini-invasive orthopedic surgery: O-arm®O2 and Surgivisio®.

Methods: The study focused on imaging of the spine. Thermoluminescent dosimeters were used to measure organs and effective doses (ED) during CBCT. An ionization-chamber and a solid-state sensor were used to measure the incident air-kerma (K_i) at the center of the CBCT field-of-view and K_i during 2D-imaging, respectively. The PCXMC software was used to calculate patient ED in 2D and CBCT configurations. The image quality in CBCT was evaluated with the CATPHAN phantom.

Results: The experimental ED estimate for the low-dose 3D-modes was 2.41 and 0.35 mSv with O-arm®O2 (Low Dose 3D-small-abdomen) and Surgivisio® (3DSU-91 images), respectively. PCXMC results were consistent: 1.54 and 0.30 mSv. Organ doses were 5 to 12 times lower with Surgivisio®. K_i at patient skin were comparable on lateral 2D-imaging (0.5 mGy), but lower with O-arm®O2 on anteroposterior (0.3 *versus* 0.9 mGy). Both systems show poor low contrast resolution and similar high contrast spatial resolution (7 line-pairs/cm).

Conclusions: This study is the first to evaluate patient ED and organ doses with Surgivisio®. A significant difference in organs doses was observed between the CBCT systems. The study demonstrates that Surgivisio® used on spine delivers approximately five to six times less patient ED, compared to O-arm®O2, in low dose 3D-modes. Doses in 2D-mode preceding CBCT were higher with Surgivisio®, but negligible compared to CBCT doses under the experimental conditions tested.

Keywords

3D surgical imaging system; Cone beam computed tomography; lumbar spine surgery; patient exposure

Abbreviations and acronyms

ABMk: fraction of active bone marrow

AP: antero-posterior

CBCT: cone beam computed tomography

CTDI: computed tomography dose index

DAP: dose-area product

DLP: dose-length product

D_{FOV}: dose to the field of view

ED: effective dose

FDD: focus to detector distance

FOV: field of view

FRD: focus to reference point distance

FSD: focus to skin distance

K_i: incident air-kerma

TLD: thermoluminescent dosimeter

Wt: tissue weighting factor

3DO: 3D Orbital

3DSU: 3D Spine universal

3D-iK-SPX1: 3D imaging Kit SPX1

1 Introduction

Navigation-assisted mini-invasive orthopedic, trauma and neuro-surgery technics have become essential all over the world. Navigation based on intraoperative 3D-imaging shows proof of increased accuracy, time saving, stressless behavior for surgeons [1-3]. Nowadays, many companies in the field of orthopedics and neurosurgery propose intraoperative CT scan to guide percutaneous trajectories as brain stereotaxy, pedicular screw insertion and vertebroplasty. Most of these imaging systems rely on cone beam computer tomography (CBCT), leading to an increased use of ionizing radiation, which raises some questions about patient exposure.

A Surgivisio® system (eCential Robotics, Gières, France) was recently acquired by our medical institution and is currently used in orthopedics departments to support spine and pelvic mini-invasive-surgery. The Surgivisio® is an innovative intraoperative C-arm, combining within a unified platform: 2D fluoroscopy, CBCT and real time navigation capabilities. The aim of this study was to evaluate patient organ doses during standard surgical procedures on spine using this new system compared to a universally used device designed for intraoperative navigation: O-arm®O2 (Medtronic, Minneapolis, MN, USA) [4-7], which has been widely characterized in terms of dosimetry [8-14]. Both systems can be used for lumbar spine surgery such as pedicular screw insertion and vertebroplasty. A direct comparison of patient radiation exposures delivered by both systems is not possible, as CBCT dosimetry is expressed in dose-area product (DAP; mGy.cm^2) for Surgivisio® and in dose-length product (DLP; mGy.cm) for O-arm®O2. The use of the effective dose (ED) allows quantifying and comparing radiation doses from diverse diagnostic procedures, using a common measure [15]. ED can be estimated using various methods: it can be calculated by applying appropriate conversion factors to DLP or DAP [16], by simulations [17] or by measurements using thermoluminescent dosimeters (TLDs) for example [18, 19]. In this study, it appeared more relevant to estimate CBCT ED using TLDs inserted in an anthropomorphic phantom. ED was also calculated with the software PCXMC [17].

The EFOMP-ESTRO-IAEA report highlights the lack of standardization of radiation dosimetry for CBCT systems [20] and proposes the use of the dose quantity D_{FOV} for “dose to the field of view” to evaluate and compare the radiation dose from CBCT devices. In our study, it was necessary to adapt the EFOMP-ESTRO-IAEA protocol, due to the configuration of the O-arm®O2 and the specific trajectory of Surgivisio®. To fully characterize the overall radiation exposure, measurements of the incident air-kerma (K_i) [21] in 2D-imaging were also performed. Finally, to obtain objective quality control parameters, the image quality in CBCT mode was evaluated using the CATPHAN phantom [20].

2 Materials and methods

2.1 The intraoperative imaging systems

The Medtronic O-arm®O2 (Figure 1A) is a mobile intraoperative X-ray system that is used worldwide for spine, cranial and orthopedics applications [4-7, 22]. It is designed for surgical procedures, pre-operative planning, interoperative imaging, and post-operative assessment. The system allows basic fluoroscopy, multi-plane 2D-imaging and 3D volumetric imaging. After 3D-imaging, O-arm®O2 can be linked to compatible image guided surgery systems. O-arm®O2's gantry contains an inner ring with a rotor unit that includes the X-ray source and a flat panel detector (Table 1). X-Y shutters are available to collimate the 2D-imaging field but also to reduce the length of the CBCT volume, they were not used in this study. O-arm®O2 provides various CBCT pre-programed clinical protocols subdivided in dose-levels for various patient thicknesses (Table 1).

Surgivisio® is an integrated operating C-arm with 2D, 3D X-ray imaging and surgical navigation [2]. Surgivisio® provides two 3D-modes: 3D Orbital (3DO) and 3D Spine universal (3DSU). 3DSU allows navigation with dedicated surgical devices. In this mode, the C-arm movement is optimized: the X-ray tube and the flat panel have an oval-like trajectory with a possible travel up to 14.0 cm in the lateral direction and 22.9 cm in the vertical direction, at maximum. As the focus to detector distance (FDD) is fixed, the center-of-rotation follows a "U-shape" trajectory. 3DSU acquisitions have to be performed with a specific device called 3D imaging Kit SPX1 (3D-iK-SPX1, Figure 1 B-C), that permits CT-reconstruction process. The X-ray tube settings (kV and mA) for 3D are automatically regulated and result from a preceding fluorography sequence (anteroposterior and lateral). The anteroposterior fluorography sequence has to be stopped by the operator when kV and mA have converged to their optimal values. Based on the 3D-iK-SPX1 position on the 2D-images, the system then calculates an optimized 3D trajectory that provides the maximal reconstructed volume: a 15-cm-in-length cylinder with an oval section (vertical axis: 16 cm, horizontal axis: 18 cm). Based on our experience, about 9 images are necessary to obtain regulated parameters from the fluorography sequence. Note that it is impossible to make repetitive CBCT without a prior fluorography sequence with Surgivisio®. The manufacturers' technical specifications and the dosimetric information provided by each system are detailed in Table 1.

2.2 Dosimetric assessment

2.2.1 Anthropomorphic Phantom

An adult female anthropomorphic phantom (model 702, CIRS Inc, Norfolk, VA, USA) was used (Figure 1). This phantom simulates a woman of 160 cm high and 55 kg in weight, according to the specifications of the International Commission on Radiological Protection [23] and the International Commission on Radiation Units and Measurements [24]. The phantom is composed of various epoxy resins, equivalent to soft tissue, bone, spinal cord, lung and brain tissues. The phantom is sectional in design, with 25 mm thick sections and provides optimized TLD locations (5 mm diameter x 25 mm long) specific to 21 radiosensitive internal organs.

2.2.2 TLD measurements

The TLDs GR207P (^{7}LiF:Mg,Cu,P) were used to evaluate and compare patient dose during CBCT with both systems. The dosimeters were calibrated in the reference irradiation facilities of the Institute for Radiological Protection and Nuclear Safety (IRSN). Dose calibration was performed with a cobalt-60 source under electron equilibrium conditions for K_i measurements. Correction factors determined at IRSN for this type of thermoluminescent powder were applied to take into account the difference in energy response of the dosimeters in spectra similar to those encountered on the studied systems. The TLDs were analyzed on a FIMEL® reader (FIMEL, Fontenay-aux-Roses, France) [25]. Measured K_i were converted to tissue kerma by applying coefficients from the reference [26]. The uncertainty of the TLD measurements was evaluated using the error propagation method described in the GUM guide [27] and was found to be 4% (one standard deviation). Note that the uncertainty from beam quality variation within the phantom was not taken into account.

2.2.3 Organ dose and effective dose computation

Tissue kerma and tissue absorbed dose were assumed to be equal. The organ dose was calculated as the mean of each TLD's tissue absorbed dose for that organ. The ED for each protocol was derived from organ doses, according to the ICRP103 methodology [28]. Doses for organs remote from the direct X-ray field were not measured by TLDs and set to zero. The active bone marrow dose was calculated, for a female aged 40, in spine (thoracic and lumbar), ribs, pelvis (sacrum and os coxae) and femur, according to the protocol described by Cristy et al. [29].

2.2.4 CBCT patient exposure

The anthropomorphic phantom was placed on a radio-transparent surgical table in the procubitus position, as shown in Figure 1. The table top surface was settled at 112 cm from the ground and the imaging systems were centered on the L4-L5 junction with 2D-modes (anteroposterior: X-ray tube under the radio-transparent couch, lateral: X-ray tube on the patient's left). 2D-imaging was acquired with low dose auto-regulated fluoroscopy and with an auto-regulated fluorography sequence, for O-arm®O2 and Surgivisio®, respectively. The resulting anteroposterior images are shown Figure 2. After the 2D-sequences, the phantom's position was precisely materialized on the couch. The phantom was opened for inserting TLDs and then carefully repositioned. For the Surgivisio® 3DSU CBCT, the 3D-iK-SPX1 was also strictly repositioned. The "Standard 3D-Medium-Abdomen" protocol was chosen to acquire CBCT with O-arm®O2. The acquisitions parameters of the different 2D and CBCT protocols are summarized in Table 2 and Table 3, respectively.

In order to obtain a better signal-to-noise ratio for each set of TLDs in the phantoms, CBCT were repeated three times with O-arm®O2. Since repetitive CBCT are not feasible with SurgiVisio® (each CBCT requires a dedicated 2D-fluorography sequence beforehand), we proceeded differently: only one CBCT was acquired, but the mA were manually set 3 times higher (*i.e.* 117 mA) than the optimized current obtained by the automatic regulation. The resulting absorbed doses for both systems were then normalized to obtain the dose equivalent to a single CBCT. For O-arm®O2, the dosimetry of the "Low Dose 3D-Small-Abdomen" protocol (120 kV, 63 mAs) was derived from that of "Standard 3D-Medium-Abdomen" protocol (120 kV, 195 mAs) by normalizing by the mAs.

2.2.5 K_i measurements during 2D-imaging

It is worth noting that 2D-imaging is not only used to locate the volume of interest before performing CBCT, but is also mandatory with Surgivisio® in 3DSU mode to calculate the optimized CBCT-parameters (kV, mA and trajectory). K_i was measured with both systems during 2D-imaging to fully characterize the overall patient exposure. Measurements were expressed as: K_i rate at 1 m, K_i rate at FSD and K_i at FSD. A solid-state sensor (DDX6-W, Radcal, Monrovia, CA, USA) designed for use in radiology and calibrated in K_i was used (accuracy ± 5%; energy dependence ± 5%).

The uncertainty on the K_i rate for both systems was calculated with the GUM method [27], taking into account the sensor uncertainty (accuracy and energy dependence), a sensor positioning error of 2 cm and the reproducibility of the measurement. It was found to be 15% and 9% with O-arm®O2® and Surgivisio®, respectively.

2.2.6 D_{FOV} measurements during CBCT

The dose to the field-of-view (FOV) called D_{FOV} is defined in the EFOMP-ESTRO-IAEA protocol [20] by equation 1:

$$D_{FOV} = K_{a,i}(FDD) \times \frac{b}{a} \times \frac{d}{c} \qquad \text{Equation 1.}$$

Where:

$K_{a,i}(FDD)$ is K_i at the FDD, measured free-in-air with a solid-state probe placed as close as possible to the imaging detector;

a is the distance from the focal spot to the isocenter;

b is the distance from the focal spot to the place of measurement;

c is the horizontal diameter of the scanned volume;

and d is the horizontal diameter of the radiation field at the place of measurement.

With the O-arm®O2, $K_{a,i}(FDD)$ cannot be measured with a solid-state dosimeter positioned on the imaging detector, because the detector is located inside the gantry (Figure 1 A) and is therefore not readily accessible [30]. We chose to adapt the EFOMP-ESTRO-IAEA methodology and directly measure the D_{FOV} with a cylindrical ion-chamber (10X6-6, Radcal, Monrovia, CA, USA), precisely positioned at the isocenter location. The ion-chamber used is intended for radiology in-beam measurements and is calibrated in K_i (accuracy ± 4%; energy dependence ± 5%). Its active volume (6 cm^3; 3.8 cm long in the longitudinal direction) was entirely irradiated during CBCT. The same approach was used with Surgivisio® in 3DO mode.

Equation 1 postulates that the isocenter is located at the FOV center, so that a is the distance to the FOV center. For Surgivisio® in the 3DSU mode, the system's isocenter is not fixed. Consequently, the distance a from the source to the FOV center is not fixed during the 180° rotation and the D_{FOV} defined previously is not accessible. A "pseudo-D_{FOV}", located at the position where all projections intersect, has been defined to evaluate the dose at the center of the FOV in this specific configuration.

The uncertainty on the D_{FOV} was calculated with the same method used for determining the uncertainty on the K_i rate. It was found to be 7% with the O-arm®O2 and 9% and 8% with Surgivisio® in 3DO and 3DSU modes, respectively.

2.2.7 PCXMC simulations

Effective doses [28] were calculated, for both 2D and 3D-imaging modes, using the commercial software PCXMC v2.0 (STUK, Radiation and Nuclear Safety Authority, Helsinki, Finland) [17], which applies Monte-Carlo methods. Simulation parameters were chosen to represent at best the experimental conditions. The 15-year-old PCXMC phantom (168.1 cm/56.3 kg) was chosen because it is the closest in size and weight to the anthropomorphic phantom used for the TLDs measurements. Since ICRP103 [28] uses the same set of tissue weighting factors for all ages, this does not affect the results and conclusions. The input parameters of PCXMC were: the X-ray tube technical specifications (machine kV, anode angle, X-ray tube filtration), the measured K_i and the irradiation field dimensions. CBCT simulations were obtained with the PCXMC Rotation program. For O-arm®O2, the simulation was performed using 360 projections (1 projection/°) and the resulting ED was normalized to the experimental conditions (391 projections). The trajectory of the Surgivisio® 3DSU was simulated as follows: the point of intersection of all projections was first defined as being the isocenter in PCXMC Rotation. For each of the 91 projections, the other parameters (FRD, beam dimensions and K_i) were then calculated taking into account the actual trajectory of Surgivisio®. Note that in the simulations the radio-transparent couch wasn't taken into account.

2.3 3D image quality assessment

CBCT image quality was assessed with the CATPHAN 600 phantom (The Phantom Laboratory, Salem, NY, USA), using the CTP528 (high resolution) and CTP515 (low contrast) modules. The phantom was hanged at the end of the couch and centered such that the system's midplane intersects the CTP515 module. The nominal slice thickness was 0.43 mm and 0.83 mm for Surgivisio® and O-arm®O2, respectively. Image quality was assessed on the mobile view station in the surgical room taking into account the nominal slice thickness. Quantitative measurements were not possible due to sizing and windowing factors applied to native images.

3 Results

3.1 Patient dose during 2D-imaging

The doses measured during the 2D-imaging sequences, which serve to locate the imaging field prior to CBCT, are shown in Table 4. In all configurations, the K_i rate delivered by Surgivisio® was found to be higher than that delivered by O-arm®O2. Factors 1.5 and 1.1 were found for skin K_i rates in the anteroposterior and lateral views, respectively (Surgivisio® *versus* O-arm®O2 ratio). As the exposure time is also longer during the anteroposterior imaging sequence of Surgivisio®, the skin K_i is about 3 times higher using Surgivisio® in comparison to O-arm®O2. In the same table are also indicated the ED calculated using PCXMC. The ED ratios were found to be in good agreement with the K_i ratios for the two orientations. The ED are about the same for both systems in the lateral view (21.2 and 21.7 µSv, for O-arm® O2 and Surgivisio®, respectively) and about 3 times higher in the anteroposterior view when using Surgivisio® (23.5 and 73.5 µSv, for O-arm®O2 and Surgivisio®, respectively). It is worth nothing that for both systems, the ED calculated by PCXMC are over-estimated in the anteroposterior view relative to the lateral view, as the radio-transparent couch was not simulated.

3.2 CBCT doses

The individual tissue doses and ED calculated during CBCT, as well as the D_{FOV} measurements are summarized in Table 5 and Table 6, respectively.

All organs considered received a lower dose using the 3DSU Surgivisio® protocol compared to the low-dose O-arm®O2 protocol. The dose ratios (Surgivisio® *versus* O-arm®O2) ranged from a minimum of 0.08 to a maximum of 0.20. The organs receiving the highest dose are the pelvis with O-arm®O2 (10.59 mGy) and the gall bladder with Surgivisio® (1.06 mGy).

The ED measured by TLDs was found to be smaller using the 3DSU Surgivisio® protocol (0.35 mSv) compared to the low-dose protocol (abdomen-small) of O-arm®O2 (2.41 mSv), ratio 0.15 (Surgivisio® *versus* O-arm®O2). PCXMC provides ED of 0.30 and 1.54 mSv, for both systems, respectively with a 0.19 ratio, in good agreement with the measurements (Table 6).

3.3 CBCT image quality

The high-contrast spatial resolution was evaluated directly on screen in the surgical room. The O-arm®O2 (16 mA/62.56 mAs/120kV/ 391 images/360°) shows comparable high contrast to Surgivisio® (39 mA/73 kV/ 91 images/180°): 7 line-pairs/cm. Neither O-arm®O2 nor Surgivisio® 3D image reveals the contrast circles present in the CTP515 low contrast CATPHAN module.

4 Discussion

To our knowledge, this is the first study evaluating patient dosimetry with Surgivio®. This mobile C-arm, used for navigation-assisted orthopedic surgery, offers an optimized partial-angle, non-isocentric trajectory for CBCT. The main finding of this study is a significant reduction (5 to 12 times) in the organs doses when using Surgivisio® compared to O-arm®O2 during CBCT for spinal surgery. Surgivisio® allows the patient to receive an ED approximately six times lower than that of O-arm®O2, using the low-dose 3D mode of each system. These findings are important for surgeons, in order to ensure the radiation protection of the patient by applying the ALARA principle [31]. The O-arm®O2 was chosen as a reference because it is used worldwide for orthopedic spine surgery applications and has already been widely described and compared [4-14]. In the Surgivisio® dosimetry report, the doses delivered during the 2D and 3D sequences are given in DAP and kerma units. On the other hand, the O-arm®O2's dosimetry reports discriminate between 2D and 3D doses, expressed respectively in DAP plus kerma units and CTDI plus DLP units. A direct comparison of doses delivered by each system during 3D-imaging was therefore not possible, based on the systems' dosimetry indicators alone (Table 3). To overcome this problem and get common measures for both systems, we chose to measure D_{FOV}, as proposed in the EFOMP-ESTRO-IAEA protocol [20] as well as organ doses and total ED measured using TLDs in an anthropomorphic phantom [15, 18, 28].

We observed different organ dose levels between both systems, but also significantly different dose distributions, as shown by organ dose ratios ranging from 0.08 to 0.20 (Surgivisio® *versus* O-arm®O2). The lowest dose ratios were observed for the pelvic, kidneys and spine. This can be explained by the non-uniform distribution of the dose with Surgivisio®, since its trajectory avoids the posterior face of the patient. Various studies have shown that partial or complete rotations lead to different dose distributions: a full-angle CBCT for imaging a homogeneous phantom led to a radially symmetrical dose gradient whereas a partial-angle irradiation leads to a non-uniform angular dose distribution [18, 32].

Significant differences in the ED levels and D_{FOV} were observed for the less irradiating CBCT protocols of both systems (Table 6). The ED estimated using TLDs for the optimized Surgivisio® protocol (3DSU) was lower than that of O-arm®O2 in low-dose mode (0.35 mSv *versus* 2.41 mSv, reduction factor of 6.9), in good agreement with the simulations (reduction factor 5.1) The difference in ED between the two CBCT systems could be mainly attributed to differences in the rotational arcs, total mAs and X-ray spectrum (kV plus filtration). Basically, the tube potential has a supralinear effect on dose: the lower tube potential used by Surgivisio® compared to O-arm®O2 (73 kV *versus* 120 kV) provides approximatively a factor of 3 in the dose reduction of Surgivisio®, as estimated by Huda et al. [33]. The

lower mAs used by Surgivisio® compared to O-arm®O2 (53 mAs *versus* 63 mAs) results in a proportional dose reduction (factor 1.18). Finally, the higher additional filtration for Surgivisio® (4.6 mm Al *versus* 4 mm Al) and the difference in rotation arcs (180° non-isocentric *versus* 360° isocentric) also contribute to a lower ED with Surgivisio®, but are more difficult to estimate approximatively.

Doses for organs outside the direct X-ray field were not measured by TLDs and set to zero to evaluate the ED. Although we may have underestimated the absolute ED, the study was not considered to be biased as the objective was to make a relative comparison between the two systems.

Numerical simulations made it possible to evaluate the ED according to the two trajectories proposed by Surgivisio®: the optimized trajectory and the isocentric trajectory. The ED obtained are only slightly different (0.31 mSv in 3DO *versus* 0.30 mSv in 3DSU) due to two compensatory effects. On the one hand, the increase of the FSD with the optimized trajectory leads to a decrease of the entrance dose, but on the other hand, the surface of the irradiated field is increased, resulting in the irradiation of a larger number of organs. It could be interesting to simulate the two CBCT modes of Surgivisio® to better characterize the influence of the Surgivisio®'s trajectories on the effective and organ doses, depending on the CBCT centering. It should be noted that O-arm®O2 offers the possibility to reduce the irradiation length by using diaphragms during CBCT whereas this option is not available with Surgivisio®.

The differences in ED values observed between TLD measurements and PCXMC calculations (2.41 *versus* 1.54 mSv, *i.e.* relative difference of 36% for O-arm®O2, and 0.35 *versus* 0.30 mSv, *i.e.* relative difference of 14 % for Surgivisio®) are inherent to the dosimetry methods and predominantly arose from differences in the phantoms used [34]. PCXMC results are strictly valid only for the phantom used for the calculation [17]. Indeed, even if we chose the closest phantom in size and weight, there is an uncertainty related to the variability of the size and location of the organs, since PCXMC uses simplistic and stylized mathematical phantoms [21, 35, 36]. The difference in ED values between PCXMC-calculations and TLD measurements was not considered to bias the relative comparison between the two systems.

As a dedicated 2D-fluorography sequence before CBCT is mandatory to obtain the optimized CBCT parameters from the AP-regulated sequence, it seemed important to compare the 2D-dosimetry of both systems. Although the fluorography rate of Surgivisio® is lower than that of O-arm®O2 (8f/s *versus* 15f/s), the 2D dosimetry was found to be higher with Surgivisio® in terms of skin K_i and ED (Table 4). K_i at patient skin were nearly identical on lateral 2D-imaging (0.5 mGy), but lower with O-arm®O2 on anteroposterior view (0.3 *versus* 0.9 mGy), compared to Surgivisio®.

Although good quality AP acquisition is necessary to obtain the optimized CBCT parameters with Surgivisio®, high image quality is not useful for lateral views that are used only for localization and could be performed with a lower dose mode, saving the overall dose delivered to the patient. Attention should be paid to the duration of the Surgivisio® fluorography sequence. If the 2D fluorography sequence is long, the ED delivered becomes non-negligible compared to the ED of 3DSU (even if it remains negligible compared to the CBCT O-arm®O2 dose).

In the clinical context of navigation-assisted minimally invasive orthopedic surgery, CBCT images are interfaced with a navigation system to provide accurate guidance of surgical instruments. In this context, the quality of CBCT clinical images is good enough for navigation and accurate screw placement, but is not comparable to CBCT or CT images for diagnostic purposes [2]. The image quality was estimated with a CATPHAN phantom. Both systems produced comparable high-contrast resolution (7 lp/mm) and neither system reveals the contrast circles present in the CTP515 low-contrast CATPHAN module. This is not surprising since both systems are intended for use when a physician benefits from 3D information from anatomical structures with high X-ray attenuation (such as bone structures and metal objects). They are not intended to be used for soft tissue imaging. The results obtained in the present study for the O-arm® O2 are comparable to those of Zhang et al [13].

With the O-arm®O2 system, it is important to note that for the same patient, the selection of the "Standard 3D-Medium-Abdomen" protocol (120 kV, 195 mAs), instead of the "Low Dose-Small–Abdomen" (120 kV, 63 mAs) results in a significant dose increase by a factor 3.1. Interestingly a potential strategy to significantly reduce the dose with the O-arm®O2 is to manually reduce the acquisition kV from 120 to 80 kV, as shown by Su et al [37].

The benefits of intraoperative imaging have been mainly demonstrated in spine surgery with increased accuracy, time savings, stressless behavior for surgeons [1-3]. Interestingly, the introduction of these mobile systems used for navigation-assisted mini-invasive orthopedic surgery also significantly reduced the doses received by the staff, as shown by Costa et al [38].

5 Conclusions

In conclusion, this study demonstrates that the effective doses received by patients using Surgivisio® for spinal surgery are significantly lower (5 to 6 times) using the optimized 3DSU sequence, compared to the least irradiating 3D protocol of O-arm®O2. In the same experimental conditions, organ doses were 5 to 12 times lower with Surgivisio® compared to O-arm®O2. These results may have implications for clinical practice when choosing interventional CBCT system for navigation-assisted surgery.

Acknowledgements

The authors would like to thank Professor J. Tonetti, A. Gaudu and the staff of the operating room of the orthopedic surgery department of the Grenoble hospital for their help in carrying out this project.

Funding

This research did not receive any specific grant from funding agencies in the public, commercial, or not-for-profit sectors.

Reference list

[1] Burstrom G, Nachabe R, Persson O, Edstrom E, Elmi Terander A. Augmented and Virtual Reality Instrument Tracking for Minimally Invasive Spine Surgery: A Feasibility and Accuracy Study. Spine (Phila Pa 1976). 2019;44:1097-104.
[2] Tonetti J, Boudissa M, Kerschbaumer G, Seurat O. Role of 3D intraoperative imaging in orthopedic and trauma surgery. Orthop Traumatol Surg Res. 2020;106:S19-S25.
[3] Vadala G, De Salvatore S, Ambrosio L, Russo F, Papalia R, Denaro V. Robotic Spine Surgery and Augmented Reality Systems: A State of the Art. Neurospine. 2020;17:88-100.
[4] Nachabe R, Strauss K, Schueler B, Bydon M. Radiation dose and image quality comparison during spine surgery with two different, intraoperative 3D imaging navigation systems. J Appl Clin Med Phys. 2019;20:136-45.
[5] Jin M, Liu Z, Liu X, Yan H, Han X, Qiu Y, et al. Does intraoperative navigation improve the accuracy of pedicle screw placement in the apical region of dystrophic scoliosis secondary to neurofibromatosis type I: comparison between O-arm navigation and free-hand technique. Eur Spine J. 2016;25:1729-37.
[6] Van de Kelft E, Costa F, Van der Planken D, Schils F. A prospective multicenter registry on the accuracy of pedicle screw placement in the thoracic, lumbar, and sacral levels with the use of the O-arm imaging system and StealthStation Navigation. Spine (Phila Pa 1976). 2012;37:E1580-7.
[7] Caire F, Gantois C, Torny F, Ranoux D, Maubon A, Moreau JJ. Intraoperative use of the Medtronic O-arm for deep brain stimulation procedures. Stereotact Funct Neurosurg. 2010;88:109-14.
[8] Uneri A, Zhang X, Yi T, Stayman JW, Helm PA, Theodore N, et al. Image quality and dose characteristics for an O-arm intraoperative imaging system with model-based image reconstruction. Med Phys. 2018;45:4857-68.
[9] Pitteloud N, Gamulin A, Barea C, Damet J, Racloz G, Sans-Merce M. Radiation exposure using the O-arm((R)) surgical imaging system. Eur Spine J. 2017;26:651-7.
[10] Su AW, McIntosh AL, Schueler BA, Milbrandt TA, Winkler JA, Stans AA, et al. How Does Patient Radiation Exposure Compare With Low-dose O-arm Versus Fluoroscopy for Pedicle Screw Placement in Idiopathic Scoliosis? J Pediatr Orthop. 2017;37:171-7.
[11] Tabaraee E, Gibson AG, Karahalios DG, Potts EA, Mobasser JP, Burch S. Intraoperative cone beam-computed tomography with navigation (O-ARM) versus conventional fluoroscopy (C-ARM): a cadaveric study comparing accuracy, efficiency, and safety for spinal instrumentation. Spine (Phila Pa 1976). 2013;38:1953-8.
[12] Abul-Kasim K, Soderberg M, Selariu E, Gunnarsson M, Kherad M, Ohlin A. Optimization of radiation exposure and image quality of the cone-beam O-arm intraoperative imaging system in spinal surgery. J Spinal Disord Tech. 2012;25:52-8.
[13] Zhang J, Weir V, Fajardo L, Lin J, Hsiung H, Ritenour ER. Dosimetric characterization of a cone-beam O-arm imaging system. J Xray Sci Technol. 2009;17:305-17.
[14] Medtronic. OARM O2 Imaging System Dosimetry Report Medtronic BI-160-00227 Rev1 2015;Version 4.0. .
[15] Brenner D, Huda W. Effective dose: a useful concept in diagnostic radiology. Radiat Prot Dosimetry. 2008;128:503-8.
[16] European Commission. European Guidance on Estimating Population Doses from Medical X-ray Procedures. Radiation Protection No 154. 2008.
[17] Tapiovaara M, Siiskonen T. PCXMC: a Monte Carlo program for calculating patient doses in medical x-ray examinations. Report STUK-A231. 2008.
[18] Kwok YM, Irani FG, Tay KH, Yang CC, Padre CG, Tan BS. Effective dose estimates for cone beam computed tomography in interventional radiology. Eur Radiol. 2013;23:3197-204.
[19] Casiraghi M, Scarone P, Bellesi L, Piliero MA, Pupillo F, Gaudino D, et al. Effective dose and image quality for intraoperative imaging with a cone-beam CT and a mobile multi-slice CT in spinal surgery: A phantom study. Phys Med. 2020;81:9-19.

[20] de Las Heras Gala H, Torresin A, Dasu A, Rampado O, Delis H, Hernandez Giron I, et al. Quality control in cone-beam computed tomography (CBCT) EFOMP-ESTRO-IAEA protocol (summary report). Phys Med. 2017;39:67-72.
[21] ICRU-74. Patient Dosimetry for X Rays Used in Medical Imaging, ICRU Rep. 74. ICRU Reports Journal of the International Commission on Radiation Units and Measurements, Bethesda, MD 2005.
[22] Medtronic. Medtronic Navigation, O-arm® O2 imaging System Version 4.0 user manual. Medtronic BI-700-02000 2015;Version 4.0. .
[23] ICRP-23. Report of the Task Group on Reference Man. ICRP Publication 23. Pergamon Press, Oxford. 1975.
[24] White DR, Buckland-Wright JC, Griffith RV, Rothenberg LN, Showwalter CK, Williams G, et al. ICRU report 48: Phantoms and Computational Models in Therapy, Diagnosis and Protection. ICRU Reports Journal of the International Commission on Radiation Units and Measurements. 1992;os25:1-194.
[25] Huet C, Entine F, Bassinet C, Dondey M, Dreuil S, Georges JL, et al. Sesame: A Tool for Numerical Dosimetric Reconstruction of Patients Overexposures in Interventional Radiology. Radiat Prot Dosimetry. 2019;185:231-8.
[26] Hubbell JH, Seltzer SM. Tables of X-Ray Mass Attenuation Coefficients and Mass Energy Absorption Coefficients. version 1.4. Gaithersburg: National Institute of Standards and Technology. 2004.
[27] BIPM. Guide to the Expression of Uncertainty in Measurement, JCGM 100:2008 (GUM 1995 with minor corrections). 2008.
[28] ICRP-103. The 2007 Recommendations of the International Commission on Radiological Protection. ICRP publication 103. Ann ICRP. 2007;37:1-332.
[29] Cristy M. Active bone marrow distribution as a function of age in humans. Phys Med Biol. 1981;26:389-400.
[30] Kenny E, Caldwell D, Lewis M. Practical radiation dosimetry across a variety of CBCT devices in Radiology. Phys Med. 2020;71:3-6.
[31] ICRP. Recommendations of the ICRP. ICRP Publication 26. Ann ICRP 1. 1977;3:1-53.
[32] Kim S, Yoo S, Yin FF, Samei E, Yoshizumi T. Kilovoltage cone-beam CT: comparative dose and image quality evaluations in partial and full-angle scan protocols. Med Phys. 2010;37:3648-59.
[33] Huda W, Scalzetti EM, Levin G. Technique factors and image quality as functions of patient weight at abdominal CT. Radiology. 2000;217:430-5.
[34] Johnson PB, Geyer A, Borrego D, Ficarrotta K, Johnson K, Bolch WE. The impact of anthropometric patient-phantom matching on organ dose: a hybrid phantom study for fluoroscopy guided interventions. Med Phys. 2011;38:1008-17.
[35] Omar A, Bujila R, Fransson A, Andreo P, Poludniowski G. A framework for organ dose estimation in x-ray angiography and interventional radiology based on dose-related data in DICOM structured reports. Phys Med Biol. 2016;61:3063-83.
[36] Borrego D, Lowe EM, Kitahara CM, Lee C. Assessment of PCXMC for patients with different body size in chest and abdominal x ray examinations: a Monte Carlo simulation study. Phys Med Biol. 2018;63:065015.
[37] Su AW, Luo TD, McIntosh AL, Schueler BA, Winkler JA, Stans AA, et al. Switching to a Pediatric Dose O-Arm Protocol in Spine Surgery Significantly Reduced Patient Radiation Exposure. J Pediatr Orthop. 2016;36:621-6.
[38] Costa F, Tosi G, Attuati L, Cardia A, Ortolina A, Grimaldi M, et al. Radiation exposure in spine surgery using an image-guided system based on intraoperative cone-beam computed tomography: analysis of 107 consecutive cases. J Neurosurg Spine. 2016;25:654-9.

Tables and Figures

Table 1

	Medtronic O-arm®O2	Surgivisio®
Technology	Mobile O-arm.	Mobile C-arm
Flat panel	40.0 x 30.0 cm^2 A-Si/CsI Varian/Paxscan® 4030D Pixel size : 0.194 mm	28.7 x 26.5 cm^2 Pixium® CsI /Thales Electron Devices/ 2630S Pixel size: 0.184 mm
Anti-scatter grid ratio	12:1	8:1
Filtration of the X-ray tube	4.0 mm Al at 75 kV	4.6 mm Al at 75 kV
Anode angle	12°	12°
Focus to detector distance	116.8 cm	115.0 cm
Focus to isocenter distance	64.7 cm	57.5 cm
Focus to reference point distance	49.7 cm	42.5 cm
2D acquisition modes:	2D fluoroscopy: 15 or 30 frame /s Multi-plane 2D	2D fluoroscopy: 1, 2, 4, 8, 12.5 frame/s 2D fluorography: 1, 2, 4, 8, 12.5 frame/s 2D radiography (one shot)
CBCT acquisition modes	Rotation: 360°, 391 projections Time: 13 s Clinical protocols (Head, extremity, chest, abdomen) subdivided in dose levels (Low Dose 3D / Standard 3D / HD3D) for various patient morphologies (S / M / L / XL)*	Rotation: 180°, 91 or 181 projections Time: 20 s <u>Trajectory:</u> a) isocentric (3D Orbital) b) optimized (3D Spine Universal)**
CBCT reconstructed volume	Volume: 21 x 21 x 16 cm^3 192 slices, 0.83 mm thickness	Maximal volume: 15-cm-in-length cylinder with an oval section vertical axis: 16 cm, horizontal axis: 18 cm 400 slices, 0.43 mm thickness
Dosimetry report	2D: Reference K_i (mGy), DAP (mGy.cm^2), Irradiation duration (s) 3D sequence: CTDIvol (mGy), DLP (mGy.cm), phantom (16 or 32)	2D and 3D sequences: Reference K_i (mGy), DAP (Gy.m^2), irradiation duration (ms)

Table 1: O-arm®O2 and Surgivisio® technical specifications.

* O-arm®O2: The kilovoltages are set to 120 kV for all torso (chest and abdomen) protocols performed with the 20 cm field of view.

** Surgivisio®: The 2D regulated fluorography sequence provides the CBCT parameters (kV, mAs and optimized trajectory).

Table 2

O-arm®O2 Low dose fluoroscopy	**Surgivisio® Fluorography**
AP imaging	AP imaging
Exposure: 67 kV, 9.4 mA	Exposure: 73 kV, 39 mA
Frame rate: 15 f/s	Frame rate: 8 f/s
FSD: 56.0 cm	FSD: 65.0 cm
Acquisition time: 1 s	Acquisition time: 2 s*
Lateral imaging	Lateral imaging
Exposure: 77 kV, 10.1 mA	Exposure: 79 kV, 44 mA
Frame rate: 15 f/s	Frame rate: 8 f/s
FSD: 51.7 cm	FSD: 58.5 cm
Acquisition time: 1 s	Acquisition time: 1 s

Table 2: Acquisition parameters for 2D-imaging sequence (AP plus Lateral) preceding 3D-imaging with O-arm®O2 and Surgivisio®. AP: antero-posterior; FSD: Focus to skin distance.

* Acquisition time for Surgivisio® anteroposterior 2D sequence was considered to be 2 s for taking into account the time needed to reach the optimized parameters (kV - mA).

Table 3

O-arm®O2 Standard-Abdomen-Medium	O-arm®O2 Low dose-Abdomen-Small	Surgivisio® 3D Orbital (3DO)	Surgivisio® 3D Spine Universal (3DSU)
Exposure: 120 kV, 50 mA, 10 ms	Exposure: 120 kV, 16 mA, 10 ms	Exposure: 73 kV, 39 mA, 15 ms	Exposure: 73 kV, 39 mA*, 15 ms
Rotation: 360°, 391 frames	Rotation: 360°, 391 frames	Rotation: 180°, 91 frames	Rotation: 180°, 91 frames
Total mAs: 195	Total mAs: 63	Total mAs: 53	Total mAs: 53
CBCT duration: 13 s	CBCT duration: 13 s	CBCT duration: 20 s	CBCT duration: 20 s
Trajectory: isocentric	Trajectory: isocentric	Trajectory: isocentric	Trajectory: optimized**
$CTDI_{vol}$: 17.13 mGy (32 cm phantom) DLP: 273.98 mGy.cm	$CTDI_{vol}$: 5.49 mGy (32 cm phantom) DLP: 87.85 mGy.cm	DAP: 108.30 cGy.cm² Reference K_i: 10.70 mGy	DAP: 108.30 cGy.cm² Reference K_i: 10.70 mGy

Table 3: Acquisition parameters for 3D X-ray imaging modes with O-arm®O2 and Surgivisio®. $CTDI_{vol}$, DAP and Reference K_i are those displayed by the two systems on the view station and in the dosimetry report.

* 3DSU parameters (kV, mA and the optimized trajectory) are those provided by the associated auto-regulated fluorography sequence.

** Optimized trajectory with 14.0 and 22.9 cm translations of the C-arm in the lateral and vertical directions, respectively.

Table 4

		Dose measurement				PCXMC simulation
		K_i rate at 1 m (mGy/min)	FSD (cm)	K_i rate at FSD (mGy/min)	K_i at skin (mGy) (Duration – frames/s)	Effective dose ICRP103 (µSv)
AP view	**O-arm®O2**	5.2	56.0	16.7	0.3 (1 s - 15 f/s)	23.5
	Surgivisio®	10.8	65.0	25.7	0.9 (2 s - 8 f/s)	73.5
	Dose Ratio Surgivisio® 3DSU / O-arm® Low dose	2.1		1.5	3.1	3.1
Lateral view	**O-arm®O2**	7.7	51.7	28.8	0.5 (1 s - 15 f/s)	21.2
	Surgivisio®	11.1	58.5	32.3	0.5 (1 s - 8 f/s)	21.7
	Dose Ratio Surgivisio® 3DSU / O-arm® Low dose	1.4		1.1	1.1	1.0

Table 4: Evaluation of 2D-imaging patient doses with O-arm®O2 and Surgivisio®: incident air-Kerma (K_i) measurements and derived effective dose calculations using PCXMC. AP view: Antero-Posterior view; FSD: focus to skin distance.

Table 5

Organ/Tissue	Number of TLDs	ABMk	Wt	Organ dose (mGy)		Organ dose ratio
				O-arm®O2 Low dose	Surgivisio® 3DSU	Surgivisio® 3DSU / O-arm® Low dose
Colon	10*		0.12	4.68	0.70	0.15
Liver	13		0.04	2.65	0.43	0.16
Lungs	2		0.12	0.39	0.06	0.16
Ovaries	2		0.08	1.06	0.12	0.11
Stomach	11		0.12	5.14	1.02	0.20
Urinary bladder	6		0.04	1.09	0.20	0.18
Active bone marrow			0.12	5.68	0.56	0.10
Femur	1	0.067		0.49	0.07	0.14
Pelvis	10	0.274		10.59	1.01	0.10
Ribs	2	0.161		1.47	0.25	0.17
Spine	6	0.284		8.83	0.85	0.10
Remainder			0.12	4.18	0.59	0.14
Adrenals	1			2.28	0.35	0.15
Gall bladder	2			5.35	1.06	0.20
Kidneys	6			7.75	0.64	0.08
Pancreas	2			6.82	1.03	0.15
Spleen	3			0.91	0.12	0.14
Uterus	3			1.45	0.20	0.13
Intestine	10*			4.68	0.70	0.15
Effective Dose (mSv)				**2.41**	**0.35**	**Ratio : 0.15**

Table 5: Organ dose for one CBCT on spine with O-arm®O2 (Low Dose 3D - small - abdomen) and Surgivisio® (3DSU - 91 images) and corresponding dose ratios (Surgivisio® *versus* O-arm®O2).

*Colon and Intestine were not distinct in the phantom; the doses were considered equal for these organs. Note: Wt: tissue weighting factor; ABMk: fraction of active bone marrow from Cristy et al. [29].

Table 6

Dosimetric value	O-arm®O2 protocol		Surgivisio® protocol		Ratio $\frac{\text{Surgivisio}^{®}\ \text{3DSU}}{\text{O-arm}^{®}\ \text{Low dose}}$
	Standard - Abdomen Medium	Low dose - Abdomen Small*	3D Orbital (3DO)	3D Spine Universal (3DSU)	
D_{FOV} (mGy) measurement at isocenter	40.5	12.9	5.1	2.9**	0.2
Effective dose (mSv) TLD measurements	7.52	2.41	-	0.35	0.15
Effective dose (mSv) PCXMC simulations	4.8	1.54	0.31	0.30	0.19

Table 6: CBCT dose with Surgivisio® and O-arm®O2: D_{FOV} measurements at the center of the field of view and effective dose estimated with TLDs or simulations. The ion-chamber was positioned at the isocenter for isocentric trajectories and at the point where all the X-ray projections intersect for the optimized trajectory of the Surgivisio®.

* The values indicated for the "Low Dose 3D - small - abdomen" protocol were calculated by normalizing the measurements obtained using the "Standard 3D - medium - abdomen" protocol with the corresponding mAs.

** With the 3DSU trajectory of the Surgivisio®, the D_{FOV} defined by the EFOMP-ESTRO-IAEA does not exist. Instead, a "pseudo-DFOV" has been defined at the center of the field of view.

Figure 1

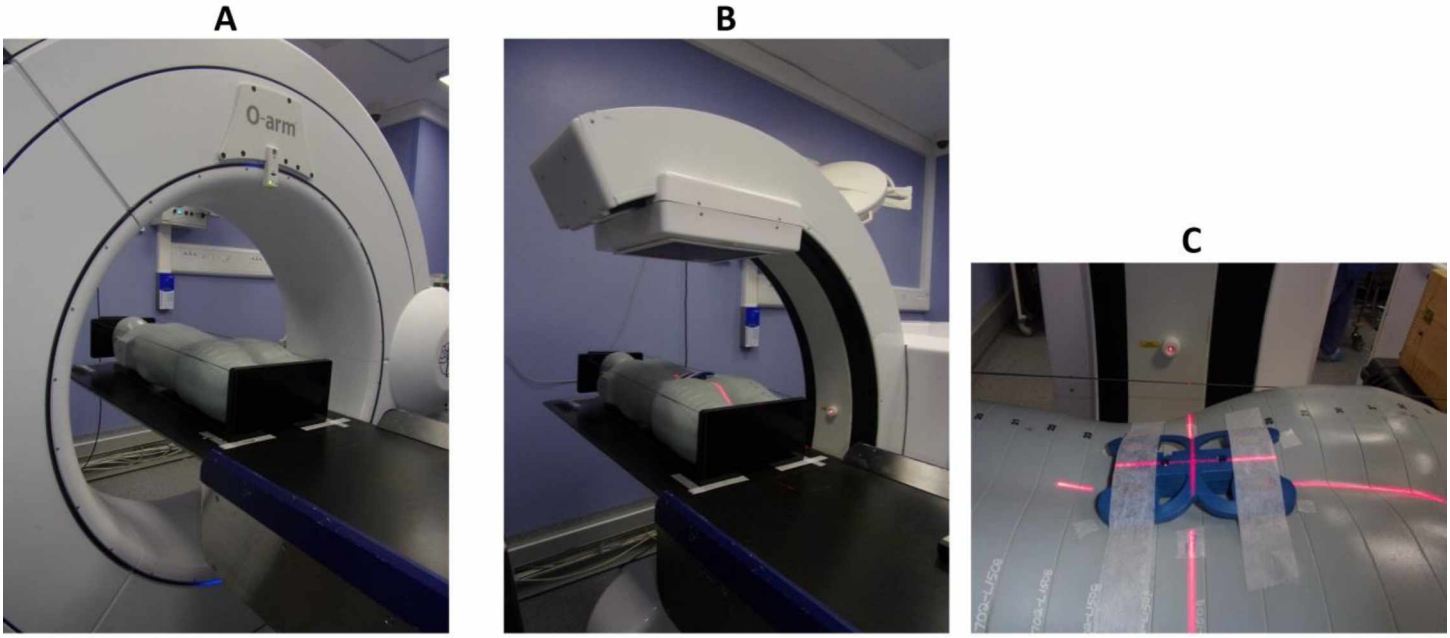

Figure 1:

A) The Medtronic O-arm®O2 and B) Surgivisio® systems in the surgery room. The same CIRS phantom and radio-transparent couch were used with the two systems. C) Focus on the blue Surgivisio® 3D imaging Kit (3D-iK-SPX1) positioned on the phantom.

Figure 2

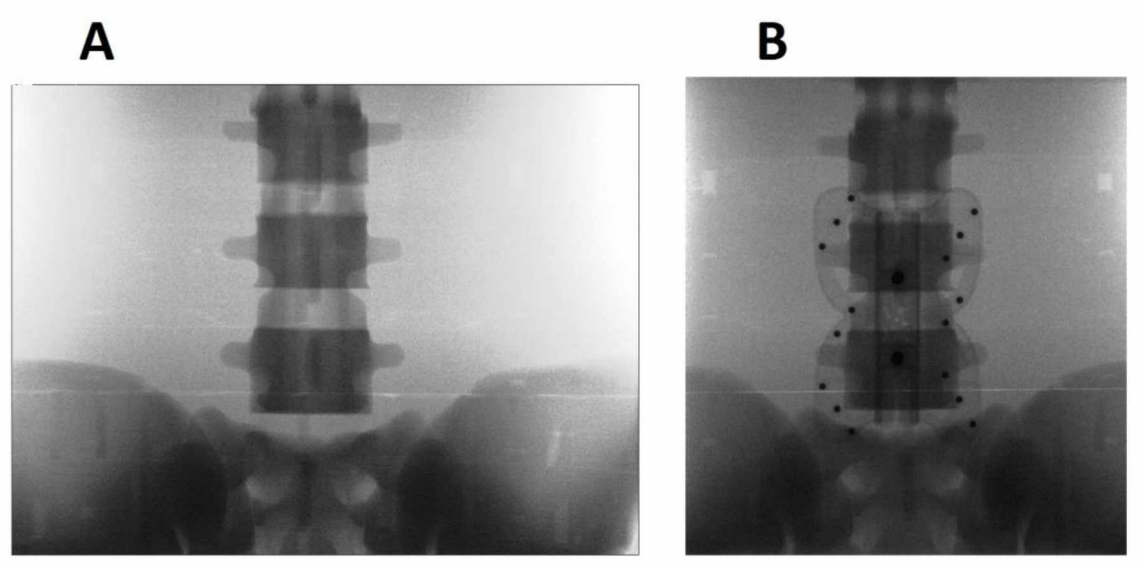

Figure 2:

Anteroposterior 2D-imaging with O-arm®O2 and Surgivisio®: localization on the L4-L5 junction before 3D. A: Last Image hold of the low-level fluoroscopy sequence with O-arm®O2. B: One image of the fluorography sequence with Surgivisio®. The 3D-iK-SPX1, positioned on the phantom spine, is visible.